Heliyon 10 (2024) e26791

Contents lists available at ScienceDirect

Heliyon

journal homepage: www.cell.com/heliyon

Research article

Targeting SLC22A5 fosters mitophagy inhibition-mediated macrophage immunity against septic acute kidney injury upon CD47-SIRPα axis blockade

Yu Jia [a,1], Jun-Hua Li [a,1], Bang-Chuan Hu [b], Xia Huang [c], Xi Yang [a], Yan-Yan Liu [a], Juan-Juan Cai [d], Xue Yang [e], Jun-Mei Lai [f], Ye Shen [f], Jing-Quan Liu [b], Hai-Ping Zhu [h], Xiang-Ming Ye [f,g,**], Shi-Jing Mo [b,f,*]

[a] *Department of Nephrology, Tongji Hospital, Tongji Medical College, Huazhong University of Science and Technology, Wuhan, 430030, Hubei, PR China*
[b] *Emergency and Intensive Care Unit Center, Intensive Care Unit, Zhejiang Provincial People's Hospital (Affiliated People's Hospital), Hangzhou Medical College, Hangzhou, 310014, Zhejiang, PR China*
[c] *Institute of Organ Transplantation, Tongji Hospital, Tongji Medical College, Huazhong University of Science and Technology, Wuhan, 430030, Hubei, PR China*
[d] *Department of Pathology, Zhejiang Provincial People's Hospital (Affiliated People's Hospital), Hangzhou Medical College, Hangzhou, 310014, Zhejiang, PR China*
[e] *Clinical Research Institute, Zhejiang Provincial People's Hospital (Affiliated People's Hospital), Hangzhou Medical College, Hangzhou, 310014, Zhejiang, PR China*
[f] *Center for Rehabilitation Medicine, Department of Intensive Rehabilitation Care Unit, Zhejiang Provincial People's Hospital (Affiliated People's Hospital), Hangzhou Medical College, Hangzhou 310014, Zhejiang, P.R.China*
[g] *Center for Rehabilitation Medicine, Rehabilitation & Sports Medicine Research Institute of Zhejiang Province, Department of Rehabilitation Medicine, Zhejiang Provincial People's Hospital (Affiliated People's Hospital), Hangzhou Medical College, Hangzhou, 310014, Zhejiang, PR China*
[h] *Department of Intensive Care Unit, The First Affiliated Hospital, Wenzhou Medical University, Wenzhou, 325000, Zhejiang, PR China*

ARTICLE INFO

Keywords:
Macrophage immune
Solute carrier family 22 member 5
Mitophagy
Septic acute kidney injury
CD47-Signal regulatory protein alpha

ABSTRACT

Efferocytosis of apoptotic neutrophils (PMNs) by macrophages is helpful for inflammation resolution and injury repair, but the role of efferocytosis in intrinsic nature of macrophages during septic acute kidney injury (AKI) remains unknown. Here we report that CD47 and signal regulatory protein alpha (SIRPα)—the anti-efferocytotic 'don't eat me' signals—are highly expressed in peripheral blood mononuclear cells (PBMCs) from patients with septic AKI and kidney samples from mice with polymicrobial sepsis and endotoxin shock. Conditional knockout (CKO) of *SIRPA* in macrophages ameliorates AKI and systemic inflammation response in septic mice, accompanied by an escalation in mitophagy inhibition of macrophages. Ablation of *SIRPA* transcriptionally downregulates solute carrier family 22 member 5 (SLC22A5) in the lipopolysaccharide (LPS)-stimulated macrophages that efferocytose apoptotic neutrophils (PMNs). Targeting SLC22A5 renders mitophagy inhibition of macrophages in response to LPS stimuli, improves survival and

* Corresponding author. Department of Intensive Rehabilitation Care Unit & Intensive Care Unit, Zhejiang Provincial People's Hospital (Affiliated People's Hospital), Hangzhou Medical College , Hangzhou, Zhejiang, 310014, PR China.
** Corresponding author. Department of Intensive Rehabilitation Care Unit & Rehabilitation Medicine, Zhejiang Provincial People's Hospital (Affiliated People's Hospital), Hangzhou Medical College, Hangzhou, Zhejiang, 310014, PR China.
E-mail addresses: yexmdr@126.com (X.-M. Ye), moshijing@hmc.edu.cn (S.-J. Mo).
[1] Yu Jia and Jun-Hua Li contribute equally to this work.

https://doi.org/10.1016/j.heliyon.2024.e26791
Received 17 May 2023; Received in revised form 19 February 2024; Accepted 20 February 2024
Available online 22 February 2024

deters development of septic AKI. Our study supports further clinical investigation of CD47-SIRPα signalling in sepsis and proposes that SLC22A5 might be a promising immunotherapeutic target for septic AKI.

Abbreviations

AKI	acute kidney injury
PMNs	neutrophils
CD47	cluster of differentiation 47
SIRPα	signal regulatory protein alpha
PBMCs	peripheral blood mononuclear cells
SLC22A5	solute carrier family 22 member 5
scRNA-seq	single-cell RNA sequencing
FACS	fluorescence-activated cell sorting
TEM	transmission electron microscopy
sg.RNA	small-guide RNA
MPO	myeloperoxidase
BMDMs	bone marrow-derived macrophages
mtROS	mitochondrial reactive oxygen species
NADH	nicotinamide adenine dinucleotide
LIE	LPS-induced endotoxemia
CLP	cecal ligation and puncture
KDIGO	kidney disease improving global outcomes

1. Introduction

Septic acute kidney injury (AKI) is a thorny health threat, with characteristic histopathology that causes mortality worldwide, highlighting the need to better understand the molecular basis of tubular damage resulting from severe infection [1,2]. Despite widespread availability of antibiotics and continuous renal replacement therapy (CRRT), the clinical prognosis in patients with septic AKI remains heterogeneous and unfavorable. Accordingly, mechanistic studies regarding septic AKI and its pathogenesis are urgent, not only to lay a framework for improving prognosis of patients with this debilitating disease, but also to gain insight into strategy that would extend effective therapies to other organ dysfunction.

Innate and adaptive immune cells, including neutrophils (PMNs), monocytes, macrophages, natural killer (NK) cells, dendritic cells (DCs) and T cells, collectively underlie the inflammatory microenvironment that has been shown to orchestrate initiation, progression and resolution of inflammation. Emerging evidence indicate that the interactions between immune and inflammatory cells are crucial to magnify the overall immune response during sepsis [3,4]. For instance, PMNs recruited at the inflammatory lesions often experience apoptosis and are cleared by macrophages through a biological process known as efferocytosis, for which receptors specifically recognizing the phagocytic signal on surface of apoptotic PMNs are required [5,6]. Supporting this notion, insufficient efferocytosis of apoptotic PMNs is found to be associated with persistence and deterioration of inflammation [7].

CD47, also known as cluster of differentiation 47 or leukocyte surface antigen CD47, is an integrin-associated transmembrane protein that functions to block phagocytosis through binding to and triggering inhibitory “don’t eat me” signal of signal regulatory protein alpha (SIRPα) in macrophages [8]. CD47-SIRPα interaction has been tightly linked to various diseases and pathological inflammatory settings such as cancer [9], liver damage [10], idiopathic pulmonary fibrosis (IPF) [11], chronic graft versus host disease [12], nonalcoholic steatohepatitis (NASH) [13] and virus infection [14]. Blockade of CD47-SIRPα signalling can lead to phagocytic removal of pathogen, epithelial cell debris, hyperproliferating fibroblasts and inflammatory proteases. Hitherto, current understanding of the possible contribution of CD47-SIRPα axis to the pathogenesis of septic AKI remains elusive.

Alterations of mitochondrial homeostasis play a pivotal role in clinical sepsis and experimental models of septic AKI [15,16]. Mitophagy control a wide range of biological processes and are delicately associated with mitochondrial dynamics and mass with temporospatial specificity. Despite considerable advancement in understanding the regulatory mechanisms for mitochondrial homeostasis, the fundamental role of mitophagy in immune cells and host defense is just beginning to be appreciated. For instance, adoptive transfer of bone marrow-derived mononuclear cells lacking mitophagy allows mice refractory to the sepsis-induced lethality [17]. On the other hand, mitophagy inhibition triggers classical macrophage activation, thereby improving survival of mice with polymicrobial sepsis [18]. However, the putative roles and mechanisms of efferocytosis in modulating macrophage mitophagy and outcome of septic AKI have not yet been shown. We therefore investigate the interplay between efferocytosis and macrophage mitophagy during septic AKI. Our data support the notion that the anti-septic AKI phenotypes due to mitophagy inhibition in

macrophages could be harnessed by CD47-SIRPα blockade as a result of transcriptional SLC22A5 downregulation through enhancing efferocytosis towards apoptotic PMNs.

2. Materials and methods

2.1. Isolation of mononuclear cells from human blood

Blood samples were collected from critically ill patients who met the clinical diagnosis of septic AKI in Zhejiang Provincial People's Hospital according to Sepsis-3 criteria [19] and Kidney Disease Improving Global Outcomes (KDIGO) score [20]. The study was conducted in accordance with the principles of the Declaration-of-Helsinki and written Informed consent was obtained from all individuals (study number: QT2022076). Human peripheral blood was retrieved in EDTA anticoagulant tubes and Ficoll-Paque PLUS (GE Healthcare) was used to obtain PBMCs for cell sorting of flow cytometry.

2.2. Cell lines and primary cultures

Murine bone-marrow-derived macrophages (BMDMs) were isolated from femurs of C57BL/6J mice at 6–10 weeks of age and cultured in Dulbecco's modified Eagle's medium (Gibco, Carlsbad, USA) supplemented with 10% fetal bovine serum (FBS), 20% L929-conditioned media and 100 U/mL penicillin/streptomycin under humidified atmosphere at 37 °C in 5% CO_2 and 95% air, and allowed to differentiate in the presence of 20 ng/mL recombinant mouse granulocyte macrophage colony-stimulating factor (GMCSF) for 7 d as previously described [21]. The detailed information for human monocyte-derived macrophages (HMDMs) and murine neutrophils (PMNs) preparation was provided in Supplemental materials and methods.

2.3. Transfection and lentivirus transduction

Plasmid transfection was carried out using Lipofectamine 3000 according to the manufacturer's instructions as described previously [22,23]. The detailed information was provided in Supplemental materials and methods.

2.4. Immunofluorescence staining

Immunofluorescence (IF) staining was performed as previously described [24]. The detailed information was provided in Supplemental materials and methods.

2.5. Fluorescence activating cell sorter (FACS) analysis

The FACS analyses of surface staining, mitochondrial mass, mitochondrial ROS, mitochondrial membrane potential ($\Delta\psi m$) and dysfunctional mitochondria were performed using a BD LSR II flow cytometer (BD Biosciences, San Jose, CA, USA) and quantified by the FlowJo V10 software (Tree Star Inc.). The detailed information was provided in Supplemental materials and methods.

2.6. Transmission electron microscopy

The procedure of transmission electron microscopy (TEM) was reported previously [21,22]. The detailed information was provided in Supplemental materials and methods.

2.7. Measurements of mitochondrial DNA (mtDNA) and NAD^+/NADH ratio

Cytosolic mtDNA was measured as previously described [25]. The detailed information was provided in Supplemental materials and methods.

2.8. Enzyme-linked immunosorbent assay

Enzyme-linked immunosorbent assay (ELISA) of sera and kidney homogenates were performed as described previously [21,22]. The detailed information was provided in Supplemental materials and methods.

2.9. RNA-sequencing (RNA-seq) and real-time quantitative PCR (RT-qPCR)

Total RNA was prepared from BMDMs of WT and $SIRPA^{CKO}$ mice subjected to CLP challenge by using RNeasy kit (Qiagen) with RNase free DNase set. Strand-specific cDNA libraries were constructed following a standard protocol and sequencing were performed using Illumina HiSeq 6000 sequencer (OEbiotech, Shanghai, China) at a paired-end run with a 100-bp read length. The expression levels of a gene were quantified by the reads per kilobase of model per million base pairs sequenced (RPKM) and the differentially expressed genes (DEGs) was defined by DEGseq algorithm. Annotation information regarding genes engaged in biological pathways was based on Reactome (https://reactome.org) and Gene Ontology (http://www.geneontology.org) databases.

The standard protocols for RT-qPCR were as described previously [23,25]. The detailed information was provided in Supplemental materials and methods.

2.10. Mice

Sirpa$^{flox/flox}$ mice were generated using the CRISPR-Cas9 system by GemPharmatech Co., Ltd. (Nanjing, China). Two *loxP* sequences were inserted in the introns flanked with *exon 2–6* of *Sirpa* as indicated in Fig. S2A. The *Lyz2-Cre* transgenic mice (Stock No. 019096) were purchased from the Jackson laboratory (Bar Harbor, ME, USA) and crossed with the *Sirpa*$^{flox/flox}$ mice for generation of *Lyz2-Cre; Sirpa*$^{flox/flox}$ (*Sirpa*^{CKO}) mice with macrophage-exclusive *SIRPA* expression. All mice were bred in a standard specific-pathogen-free environment in accordance with institutional and NIH guidelines and all animal procedures have been approved by the Institutional Animal Care and Use Committee of Hangzhou Medical College.

2.11. Animal experiments

Murine models of LPS-induced endotoxemia (LIE) and cecal ligation and puncture (CLP) were established as described previously [22,26,27]. The detailed information was provided in Supplemental materials and methods.

2.12. Myeloperoxidase (MPO) assay

MPO assay was performed by Myeloperoxidase Colorimetric Activity Assay Kit (BioVision, Mountain View, CA) according to manufacturer's protocol. Briefly, kidney tissues were homogenized in 1 mL PBS and sonictaed for 15 min, followed by homogenizing in 200 μL of MPO assay buffer secondly and centrifuging at 15,000 rpm for 5 min. MPO activity of the supernatant was then measured at 450 nm by a colorimetric microplate reader and calculated as the change in absorbance per sample.

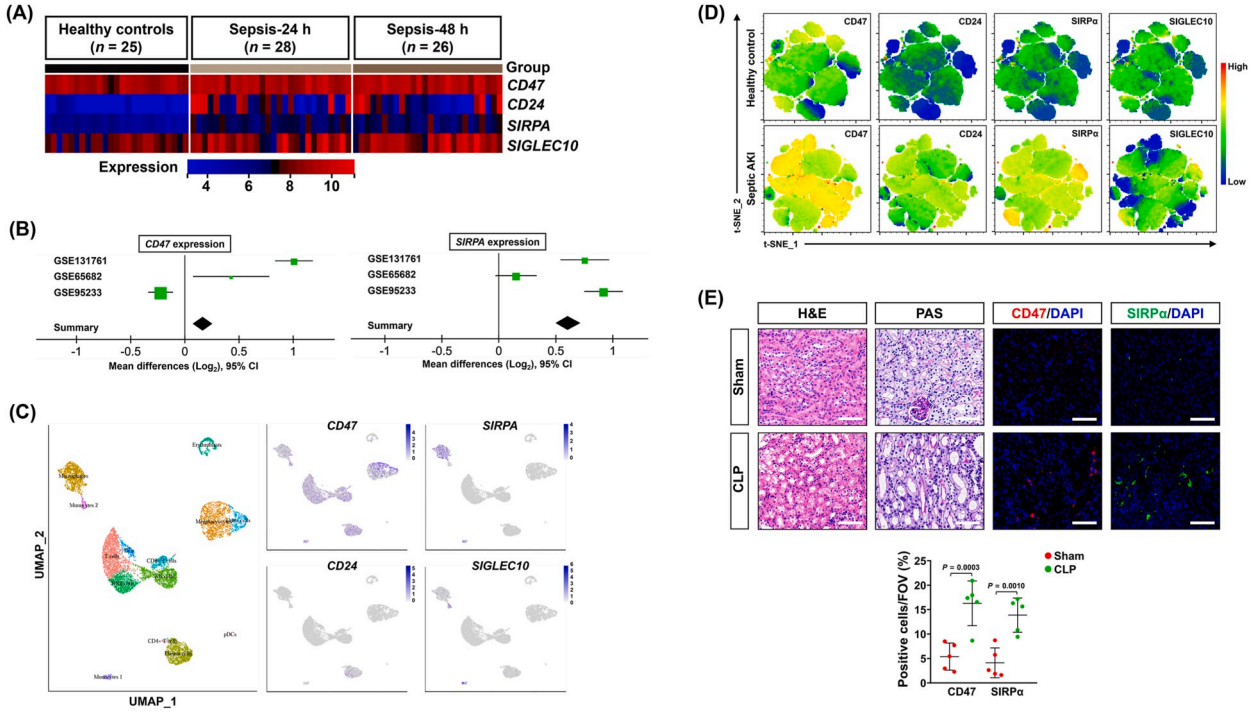

Fig. 1. CD47 and SIRPα are highly expressed in septic AKI. (A) Heat map showing *CD47* and *SIRPA* gene expression in the publicly available dataset (GSE57065) from the NCBI GEO as compared to the known anti-efferocytotic immune checkpoints *CD24* and *SIGLEC10*. (B) Meta-analysis denoting odds ratio (OR) of *CD47* and *SIRPα* expression levels in three GEO datasets of septic patients as indicated. (C) Uniform manifold approximation and projection (UMAP) plots of cell clusters as well as *CD47*, *SIRPA*, *CD24* and *SIGLEC10* expression in the scRNA-seq data from GSE167363. (D) Multicolour flow cytometric analyses of t-SNE plots showing the distribution of CD47, SIRPα, CD24 and SIGLEC10 in PBMCs of patients with septic AKI. (E) Representative images for hematoxylin and eosin (H&E), periodic acid-Schiff (PAS) and immunofluorescence (IF) staining of CD47 and SIRPα in renal sections from cecal ligature and puncture (CLP) mice ($n = 5$). Scale bar = 50 μm. Data are expressed as mean ± s.d. (E). Two-sided ANOVA with Bonferroni post hoc *t*-test correction was used to calculate the *P* value (E).

2.13. Macrophage elimination and adoptive transfer studies

Macrophages were eliminated by the commercially available clodronate liposomes (www.clodronateliposomes.com) using an intravenous (i.v.) delivery method as indicated previously [21]. The detailed information was provided in Supplemental materials and methods.

2.14. Meta-analysis of public sepsis data sets

For gene expression studies, raw data of GSE131761, GSE65682 and GSE95233 were downloaded from the Gene Expression Omnibus (GEO) database (http://www.ncbi.nlm.nih.gov/geo/). After re-annotating the probes, each data set was normalized using MAS 5.0 algorithm with $\log_2$ transformation. Meta-analysis were performed using RevMan 5.3 software provided by www.cochrane.org, with Z-statistics as a ratio of the pooled effect size to its standard error for each gene.

2.15. Quantification and statistical analyses

The gene expression and cell type annotation of RNA-sequencing data from peripheral blood samples of septic shock patients (GSE57065) and scRNA-sequencing data from peripheral blood mononuclear cells (PBMCs) of patients with systemic gram-negative bacterial sepsis (GSE167363) were downloaded from the Gene Expression Omnibus. Seurat (version 2.3.2) were used to process single-cell RNA-seq data following the standard procedure. Data were analyzed using GraphPad Prism software version 8.0 (La Jolla, CA, USA) and were presented as the mean ± s.d. of at least three independent experiments. Log-rank test with adjustment for ties based on mid-ranks was used for statistical evaluation of all survival curves. Two-tailed unpaired *t*-test was utilized for comparing means from two groups of data unless otherwise stated. For comparing more than two groups with assumed normal distributions, two-sided ANOVA was carried out followed by Bonferroni post-hoc *t* tests. $P < 0.05$ was considered statistically significant as indicated in the figure legends.

3. Results

3.1. CD47 and SIRPα are highly expressed in septic AKI

To evaluate the role of CD47-SIRPα signalling in regulating the macrophage-mediated immunity during septic AKI, we examined the expression of CD47 and SIRPα in diverse sepsis cases. RNA-sequencing data from publicly available transcriptional profiling datasets deposited in Gene Expression Omnibus (GEO) website [28] identified high expression of *CD47* and *SIRPA* in nearly all peripheral blood specimens of patients in conjunction with the robust upregulation of known anti-efferocytotic immune checkpoints *CD24* and sialic acid binding Ig like lectin-10 (*SIGLEC10*) (Fig. 1A and Fig. S1A). Using a formal meta-analysis of four datasets from blood samples of septic patients versus their individual non-septic subjects, we observed an overall odds ratio (OR) of 0.17 (95% confidence interval [CI]: 0.08–0.26) for *CD47* expression and 0.61 (95% confidence interval [CI]: 0.50–0.72) for *SIRPA* expression (Fig. 1B). When determining *CD47* and *SIRPA* expression in peripheral blood mononuclear cells (PBMCs) of patients subjected to systemic Gram-negative bacterial sepsis by single-cell RNA sequencing (scRNA-seq) data [29], we found that PBMCs expressed high levels of *CD47*, which were substantially broader than *CD24*. In contrast, *SIRPA* expression was strong in a fraction of monocytes and macrophages but was weak in other cell clusters (Fig. 1C). The significance of *CD47* and *SIRPA* upregulation for sepsis in the meta-analysis and scRNA-seq data was further evidenced by our multicolour flow cytometric analyses showing that both *CD47* and *SIRPA* were highly expressed in PBMCs of patients with septic AKI as compared to those of healthy volunteers (Fig. 1D). These findings together suggest that upregulation of CD47 and SIRPα in immune cells could be a common feature in sepsis with different pathoetiologies.

In concert with the dose-dependent elevation in protein abundance (Fig. S1B), fluorescence-activated cell sorting (FACS) identified prominent upregulation of SIRPα in the LPS-stimulated primary murine bone marrow-derived macrophages (BMDMs) (Fig. S1C). These observations were in line with transcriptomic data [30] showing that the monocyte-derived macrophages (MDMs) from human PBMCs expressed higher levels of *SIRPA* following LPS stimuli (Fig. S1D). We then examined CD47 and SIRPα expression in murine kidneys from two experimental models of sepsis: cecal ligature and puncture (CLP) and LPS-induced endotoxemia (LIE). It is noteworthy that the $CD47^+$ and $SIRP\alpha^+$ cells were almost undetectable in kidneys derived from either sham or control mice, but they profoundly accumulated in renal sections derived from CLP and LIE mice that were characterized by hallmarks of AKI, including tubular vacuolization, loss of epithelial brush border and desquamation, as well as altered counts of peripheral monocytes and neutrophils (PMNs) (Fig. 1E, Fig. S1E, S2A and B). These data support the notion that levels of CD47 and SIRPα are upregulated in septic AKI with different origins.

3.2. Interruption of CD47-SIRPα signalling governs the macrophage-mediated immunity against septic AKI

To decipher the immune roles of CD47 and SIRPα in pathogenesis of septic AKI, we generated macrophage-specific *SIRPA* knockout (KO) mice (hereinafter termed as $SIRPA^{CKO}$) (Fig. S2A), which was validated by the absence of SIRPα colocalization with macrophages from the dichromatic immunofluorescence staining of SIRPα and F4/80 in renal sections as compared to the wild-type (WT) mice (Fig. S2B). To delineate whether CD47-SIRPα signalling contributes to the development of septic AKI, we subjected $SIRPA^{CKO}$ mice and

their corresponding wild-type (WT) littermates to CLP. Although *SIRPA*^{CKO} mice had comparable renal morphology to WT mice at health status, they displayed significantly compromised kidney injury following CLP challenge (Fig. 2A). In parallel, serum creatinine—a marker of glomerular permeability, and cystatin C—an indicator of tubular damage, were lower in *SIRPA*^{CKO} mice subjected to CLP relative to WT littermates while were similar in the sham-operated *SIRPA*^{CKO} mice and WT mice (Fig. 2B and C). Given release of MPO from apoptotic neutrophils (PMNs) is associated with nephrotoxicity mediated by reactive oxygen species (ROS) [31], we analyzed myeloperoxidase (MPO) activity in renal tissues and found that *SIRPA*^{CKO} mice had decreased MPO activity in comparison to WT mice following CLP operation (Fig. 2D). These data thus demonstrate a potential role for macrophage SIRPA deficiency in protection against septic AKI by counteracting MPO release.

Efferocytosis of apoptotic PMNs by macrophages facilitate inflammation resolution [32]. Upon CLP surgery, coimmunostaining of Ly6G and F4/80 in renal sections from WT mice demonstrated that macrophages engulfed PMNs, and this phenomenon became more evident in *SIRPA*^{CKO} mice (Fig. 3A). Co-localization of Ly6G was predominantly found in the MHCII^{+} macrophages, but not in the CD206^{+} macrophages within septic AKI lesions (Figs. S3A and B). An independent *in vivo* efferocytosis assays using flow cytometry with F4/80 and CMFDA staining further revealed that SIRPA deficiency significantly increased percentage of peritoneal macrophages (PMs) that efferocytose CMFDA^{+} apoptotic PMNs in response to CLP challenge (Fig. S3C). We therefore measured cytokines of innate immune system in kidneys and sera from both *SIRPA*^{CKO} and WT mice following CLP surgery and found that the production of pro-inflammatory cytokines in *SIRPA*^{CKO} mice were less than those of WT littermates (Fig. 3B and C). These results indicate that blockade of CD47-SIRPα signalling renders the macrophage-mediated efferocytosis for inflammation resolution during septic AKI.

3.3. Interruption of CD47-SIRPα signalling escalates mitophagy inhibition of macrophages during septic AKI

To understand the general impact of efferocytosis on macrophages triggered by CD47-SIRPα blockade, we performed RNA sequencing (RNA-Seq) in bone marrow-derived macrophages (BMDMs) isolated from WT and *SIRPA*^{CKO} mice subjected to CLP challenge. Gene Ontology (GO) and Reactome pathway analyses identifed the top 20 of differentially expressed genes that were significantly enriched in distinct biological processes including cellular response to oxidative stress and regulation of mitochondrial memebrane potential (Δψm) (Fig. 4A). To verify this, we harvested PMNs and exposed them to 1% FBS-supplemented Hank's Balanced Salt Solution (HBSS) overnight for apoptosis induction (Fig. S4A), followed by coincubation with WT or *SIRPA*^{CKO} BMDMs under LPS stimuli. We observed that *SIRPA*^{CKO} BMDMs engulfed apoptotic PMNs to a much stronger degree than WT BMDMs did (Fig. S4B); they concomitantly displayed an increase in mitochondrial reactive oxygen species (mtROS) production as reflected by MitoSox Red staining (Fig. 4B, left panel). However, incubating of BMDMs with apoptotic PMNs and in a Transwell system or utilizing conditioned medium (CM) from apoptotic PMNs to treat BMDMs barely influenced mtROS production of BMDMs regardless of *SIRPA* deficiency (Figs. S4C and D). Notably and in accordance with this finding, TMRM staining revealed a significantly greater amount of Δψm in the

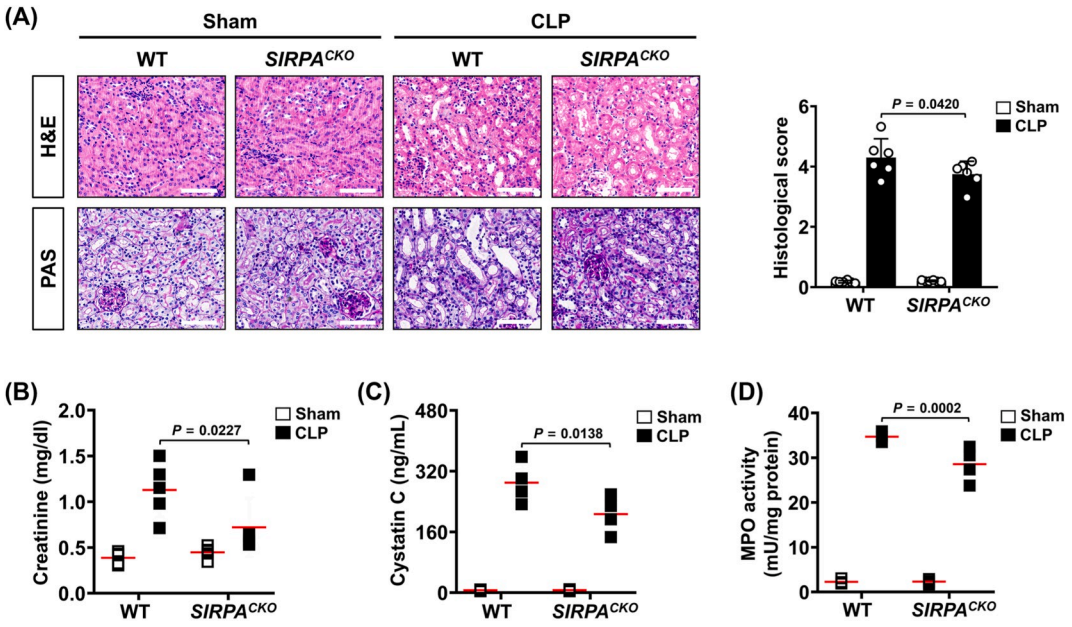

Fig. 2. Macrophage-specific knockout (KO) of *SIRPA* protects against septic AKI. (A) Representative hematoxylin and eosin (H&E) and periodic acid-Schiff (PAS) images of renal sections from wild-type (WT) and *SIRPA*^{CKO} mice with cecal ligature and puncture (CLP) challenge. Scale bar = 50 μm. (B and C) Serum creatinine (B) and cystatin C (B) levels of wild-type (WT) and *SIRPA*^{CKO} mice with cecal ligature and puncture (CLP) challenge ($n \geq 4$). (D) Myeloperoxidase (MPO) activity of renal tissues in wild-type (WT) and *SIRPA*^{CKO} mice with cecal ligature and puncture (CLP) challenge ($n \geq 4$). Data are expressed as mean ± s.d. (A–D). Two-sided ANOVA with Bonferroni post hoc *t*-test correction (A–D) was used to calculate the *P* value.

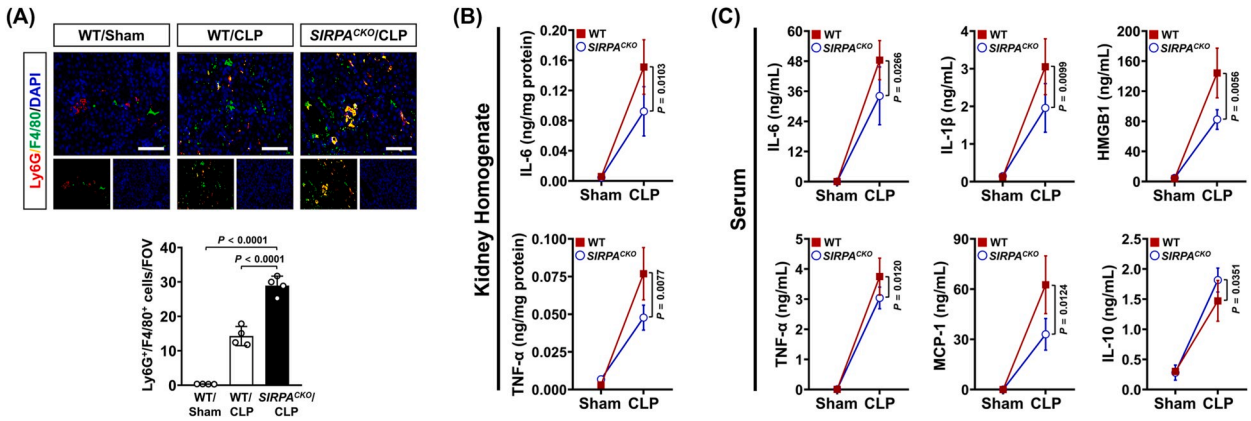

Fig. 3. Macrophage-specific knockout (KO) of *SIRPA* governs the macrophage -mediated efferocytosis for inflammation resolution. (A) Dichromatic immunofluorescence staining and proportion of Ly6G and F4/80 in renal sections from wild-type (WT) and $SIRPA^{CKO}$ mice with cecal ligature and puncture (CLP) challenge ($n = 4$). (B) ELISA assays testing interleukin-6 (IL-6) and tumor necrosis factor-α (TNF-α) in kidney homogenate of wild-type (WT) and $SIRPA^{CKO}$ mice with sham or cecal ligature and puncture (CLP) challenge ($n \geq 4$). (C) ELISA assays measuring interleukin-6 (IL-6), interleukin-1β (IL-1β), high mobility group box 1 (HMGB1), tumor necrosis factor-α (TNF-α), monocyte chemoattractant protein-1 (MCP-1) and interleukin-10 (IL-10) production in sera of wild-type (WT) and $SIRPA^{CKO}$ mice with sham or cecal ligature and puncture (CLP) challenge ($n \geq 3$). Data are expressed as mean ± s.d. (A–C). Two-sided ANOVA with Bonferroni post hoc *t*-test correction (A–C) was used to calculate the *P* value.

LPS-stimulated $SIRPA^{CKO}$ BMDMs with apoptotic PMNs coincubation in comparison to the stimulated WT BMDMs with apoptotic PMNs coincubation or the $SIRPA^{CKO}$ BMDMs without coincubation (Fig. 4B, right panel). Pretreatment with cytochalasin D, an actin polymerization inhibitor that blocks ingestion of apoptotic PMNs, however, eventually abrogated the elevation of Δψm in efferocytic $SIRPA^{CKO}$ BMDMs (Fig. S4E).

mtROS production and Δψm alteration are linked to mitophagy [33]. In support of this, $SIRPA^{CKO}$ BMDMs contained a higher amount of mitochondrial mass as reflected by MitoTracker Green staining of FACS than WT BMDMs in CLP mice (Fig. 4C and Fig. S5A). Transmission electron microscopy (TEM) corroborated a reduction in mitophagosome of the CLP-challenged $SIRPA^{CKO}$ BMDMs (Fig. 4D). In primary mouse peritoneal macrophages (PMs) from the efferocytic coculture systems under LPS stimuli, depleting *SIRPA* with short hairpin RNA (sh.RNA) favored release of fragmented mtDNA to cytosol but circumvented NAD^+/NADH ratio (Fig. 4E, F and S5B). The *SIRPA*-deficient PMs, however, had comparable mtDNA levels and NAD^+/NADH ratio to the stimulated *SIRPA*-proficient cells in the absence of apoptotic PMNs coincubation, suggesting that the mitophagy-inhibitory role of *SIRPA* deficiency in macrophages are presented only in the case of efferocytosis. To elucidate whether pharmacological blockade of CD47-SIRPα signalling influences mitophagy of PMs *in vivo*, we chose to use MIAP410, an anti-CD47 mAb that that had been shown to fully block the *in trans* CD47 interaction with SIRPα without interfering with the *in cis* CD47-β2 integrin interaction [34]. Administering MIAP410 led to a remarkable increase in population of the $MHCII^+$ PMs with high mitochondrial mass in CLP mice, yet had minimal effects on those in sham mice (Fig. S6). Thus, blockade of CD47-SIRPα signalling enhances efferocytosis for mitophagy inhibition in macrophages during septic AKI.

In further *in vitro* experiments, we depleted *SIRPA* gene in J774 macrophages and transfected them with pDsRed2-Mito vector that allows fluorescent labeling of mitochondria before coincubation with apoptotic PMNs in the context of LPS stimuli (Fig. S7A). We observed diminished fluorescence intensity in the *SIRPA*-depleted J774 macrophages when compared with the *SIRPA*-intact J774 macrophages (Fig. S7B). We then measured the spectral shift of mitochondrial-targeted mKeima (mt-mKeima) by establishing a J774 macrophage line stably expressing mt-mKeima-cox8, whose fluorescence emitted is converted by the Keima protein. Determination of the replacement of green fluorescence by red fluorescence, a quantitative method for reflecting mitophagic activity, showed an impaired replacement in the *SIRPA*-depleted J774 macrophages (Fig. 4G). Mitochondrial recruitment of PINK1 is a hallmark of mitophagy [35]. We determined the colocalization of PINK1 with mitochondrion outer membrane protein TOMM20 in the LPS-stimulated J774 macrophages with apoptotic PMNs coincubation and found that the recruitment of PINK1 into mitochondria was impeded after *SIRPA* depletion (Fig. S7C).

To explore the translation of these findings to human pathology, we tested whether interruption of CD47-SIRPα signalling could alter mitochondrial homeostasis of human monocyte-derived macrophages (HMDMs) through confering efferocytosis towards apoptotic human neutrophils (HPMNs). To this end, we used a small-guide RNA (sg.RNA) to target the *SIRPA* locus, which markedly knocked out SIRPα expression relative to control sg. RNA (sg.Ctrl) after introduction for three days (Fig. S8A). Of note, transduction of sg. *SIRPA* potentiated the efferocytic ability of HMDMs and increased their mtROS production under LPS stimuli (Figs. S8B and C). We then hypothesized that the increased mtROS in the efferocytotic HMDMs upon *SIRPA* KO could be due to accumulation of dysfunctional mitochondria. To address this issue, we performed flow cytometry with a combination of MitoTracker Green (Δψm-independent mitochondrial stain) and MitoTracker Red (Δψm-dependent mitochondrial stain). *SIRPA* KO increased dysfunctional mitochondria of the efferocytotic HMDMs but failed to do so in the non-efferocytotic HMDMs (Fig. 4H).

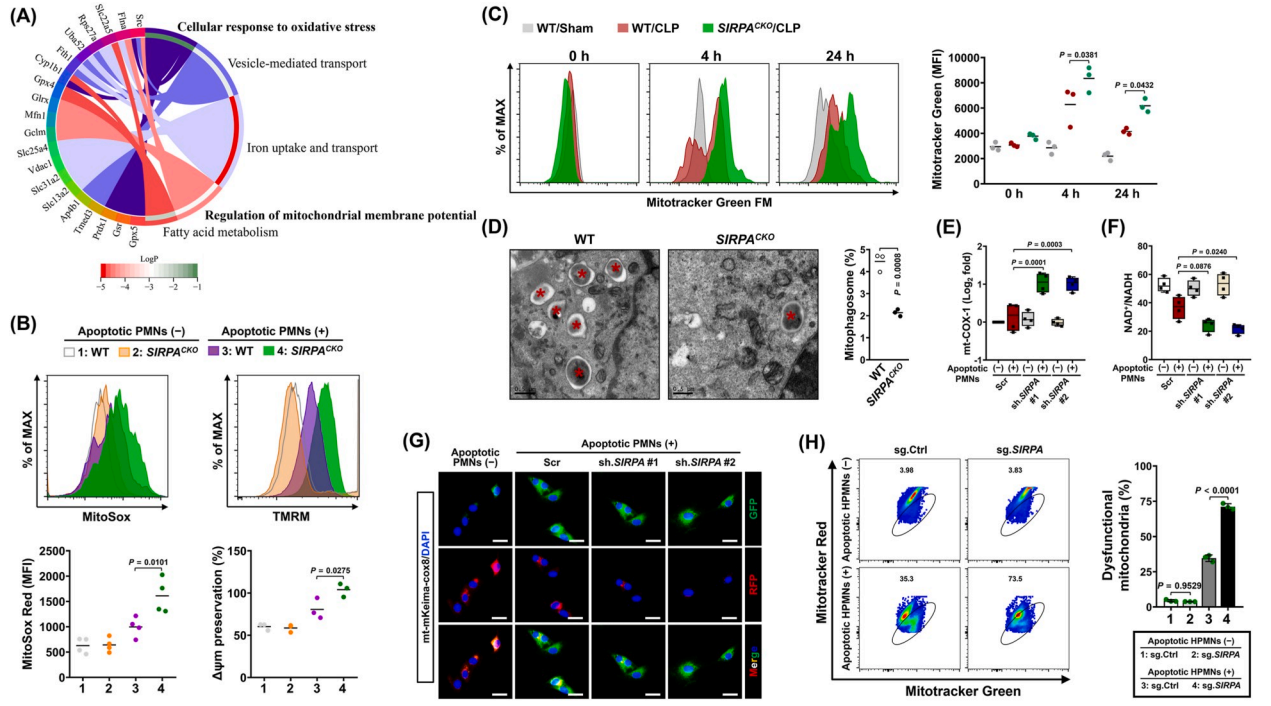

Fig. 4. Ablation of *SIRPA* escalates mitophagy inhibition of macrophages during septic AKI. (A) Chord diagram showing enriched biological processes based on Gene Ontology (GO) and Reactome pathway analyses for top 20 differentially expressed genes (DEGs) in RNA-seq datasets of bone marrow-derived macrophages (BMDMs) from WT and *SIRPA*^{CKO} mice subjected to cecal ligature and puncture (CLP). (B) Histogram plots and quantification of flow cytometry with MitoSox Red (left panel) and TMRM (right panel) staining for measurement of mitochondrial reactive oxygen species (mtROS) and mitochondrial membrane potential (Δψm) in WT and *SIRPA*^{CKO} bone marrow-derived macrophages (BMDMs) coincubated with apoptotic neutrophils (PMNs) in the presence of LPS (150 ng/mL) stimuli (n = 4 and 3). (C) Histogram plots and quantification of flow cytometry with MitoTracker Green staining for measurement of mitochondrial mass in bone marrow-derived macrophages (BMDMs) from WT and *SIRPA*^{CKO} mice subjected to cecal ligature and puncture (CLP) challenge at the indicated times, respectively (n = 3). (D) Representative images and quantification of transmission electron microscopy (TEM) examining mitophagosome (indicated by asterisk) in bone marrow-derived macrophages (BMDMs) from WT and *SIRPA*^{CKO} mice subjected to cecal ligature and puncture (CLP) challenge (n = 3). Scale bar = 0.5 μm. (E) RT-qPCR determining cytosolic release of mitochondrial COX-1 (mt-COX-1) in the LPS-stimulated primary mouse peritoneal macrophages (PMs) after introduction of short hairpin RNA (sh.RNA) targeting scrambled (Scr) or *SIRPA* (sh.*SIRPA*) in the presence of apoptotic neutrophils (PMNs) coincubation (n = 4). (F) NAD^+/NADH ratio of the LPS-stimulated primary mouse peritoneal macrophages (PMs) after introduction of short hairpin RNA (sh.RNA) targeting scrambled (Scr) or *SIRPA* (sh.*SIRPA*) in the presence of apoptotic neutrophils (PMNs) coincubation (n = 4). (G) Immunofluorescence images of the LPS-stimulated J774 macrophages with mt-mKeima-cox8 plasmid transfection after introduction of short hairpin RNA (sh.RNA) targeting scrambled (Scr) or *SIRPA* (sh.*SIRPA*) in the presence or absence of apoptotic neutrophils (PMNs) coincubation. GFP, green fluorescence protein. RFP, red fluorescence protein. Scale bar = 25 μm. (H) Pseudocolor plots and quantification of flow cytometry measuring dysfunctional mitochondria in sg. *SIRPA*-transfected human monocyte-derived macrophages (HMDMs) with apoptotic human neutrophils (HPMNs) coincubation coincubation in the presence of LPS stimuli (n = 3). Data are expressed as mean ± s.d. (B–F, H). Unpaired, two-tailed Student's t-test (D) and two-sided ANOVA with Bonferroni post hoc t-test correction (B, C, E, F and H) was used to calculate the P value, respectively. (For interpretation of the references to colour in this figure legend, the reader is referred to the Web version of this article.)

3.4. Blockade of CD47-SIRPα signalling inhibits mitophagy of efferocytotic macrophages through downregulating SLC22A5

Efferocytosis predominates solute carrier family of membrane transport proteins (SLCs) in macrophages [36]. We hypothesized that certain SLCs might be involved in the inhibitory role of CD47-SIRPα blockade in mitophagy of efferocytotic macrophages. To test this possibility, we compared SLC transcripts in *SIRPA*^{CKO} versus WT BMDMs from the CLP-challenged mice and identified *SLC31A2* and *SLC22A5*—the Copper and carnitine transporters responsible for copper ion transmembrane transport and L-carnitine uptake—as two mostly downregulated genes (Fig. 5A). We therefore tried to clarify this finding by conducting RT-qPCR and western-blotting, which showed that *SLC31A2* and *SLC22A5* mRNA and protein levels were lower in *SIRPA*^{CKO} BMDMs than in WT BMDMs of CLP mice (Figs. S9A and B). To further assess the effect of CD47-SIRPα blockade on *SLC31A2* and *SLC22A5* genes, the *SIRPA*-depleted PMs were coincubated with apoptotic PMNs under LPS stimuli. Both *SLC31A2* and *SLC22A5* expression were reduced in the *SIRPA*-depleted PMs with apoptotic PMNs coincubation but remained statistically unchanged in those without (Fig. 5B). The downregulation of SLC31A2 and SLC22A5 at protein levels were also confirmed in efferocytotic PMs with LPS stimuli after depleting *SIRPA* (Fig. 5C). In the LPS-stimulated HMDMs efferocytosis coculture system, sg. *SIRPA* suppressed mRNA and protein levels of SLC22A5 (Fig. 5D and E). These results depict that the CD47-SIRPα blockade-dependent efferocytosis may be well-positioned to affect biological roles of

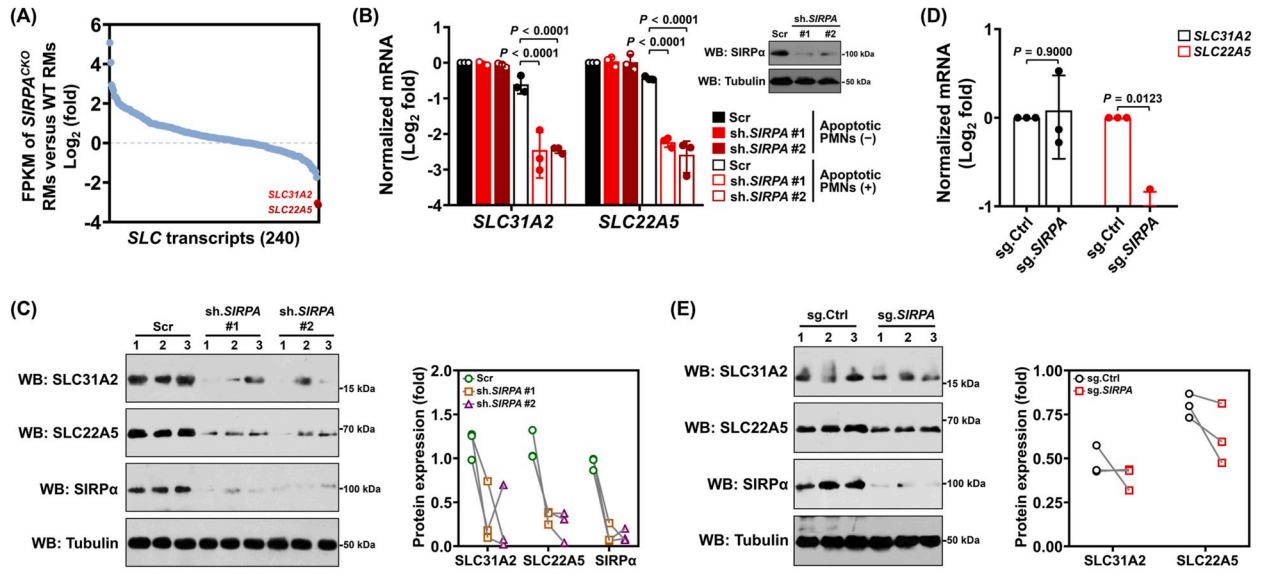

Fig. 5. Blockade of CD47-SIRPα signalling downregulates SLC31A2 and SLC22A5 in efferocytotic macrophages in response to LPS stimuli. (A) Fold changes of *SLC* transcripts in *SIRPA*^{CKO} versus WT bone marrow-derived macrophages (BMDMs) from mice subjected to cecal ligature and puncture (CLP) challenge. (B) RT-qPCR comparing *SLC31A2* and *SLC22A5* mRNA expression in LPS-stimulated primary mouse peritoneal macrophages (PMs) with apoptotic neutrophils (PMNs) coincubation after introduction of short hairpin RNA (sh.RNA) targeting scrambled (Scr) or *SIRPA* (sh.*SIRPA*) ($n = 3$). Insert: Western-blotting (WB) analyses examining SIRPα expression in primary mouse peritoneal macrophages (PMs) transfected with shRNA targeting scrambled (Scr) or *SIRPA* (sh.*SIRPA*). (C) Western-blotting (WB) analyses assessing SLC31A2 and SLC22A5 abundance in LPS-stimulated primary mouse peritoneal macrophages (PMs) with apoptotic neutrophils (PMNs) coincubation after introduction of short hairpin RNA (sh.RNA) targeting scrambled (Scr) or *SIRPA* (sh.*SIRPA*) ($n = 3$). (D and E) RT-qPCR (D) and western-blotting (WB) analyses (E) measuring mRNA and protein expression of SLC31A2 and SLC22A5 in sg. *SIRPA*-transfected human monocyte-derived macrophages (HMDMs) with apoptotic human neutrophils (HPMNs) coincubation in the presence of LPS stimuli ($n = 3$). Data are expressed as mean ± s.d. (B and D). Two-sided ANOVA with Bonferroni post hoc *t*-test correction (B) and Unpaired, two-tailed Student's *t*-test (D) was used to calculate the *P* value, respectively.

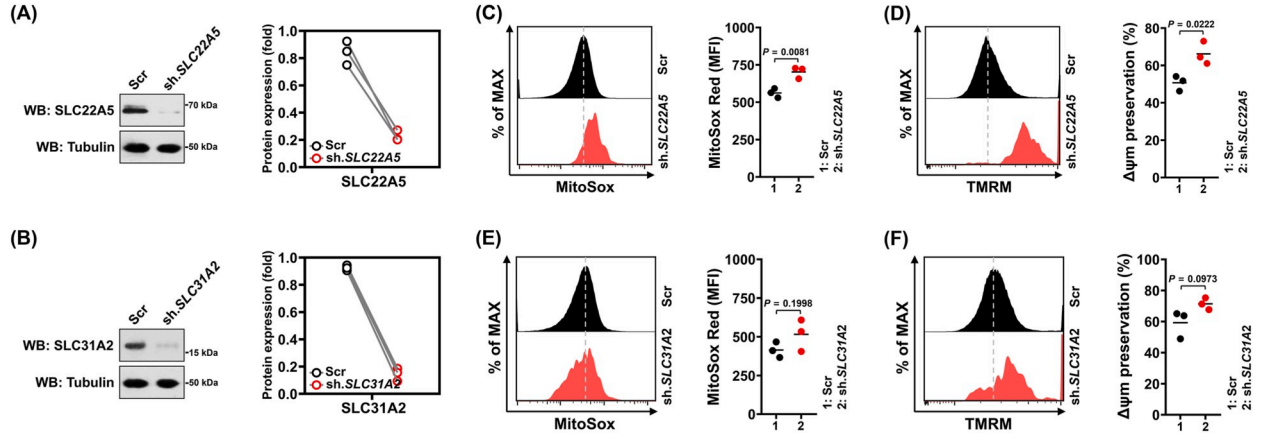

Fig. 6. Depletion of SLC22A5, but not SLC31A2, inhibits mitophagy of macrophages under LPS stimuli. (A) Western-blotting (WB) analyses determining SLC22A5 abundance in bone marrow-derived macrophages (BMDMs) transfected with shRNA targeting scrambled (Scr) or *SLC22A5* (sh.*SLC22A5*). (B) Western-blotting (WB) analyses examining SLC31A2 abundance in bone marrow-derived macrophages (BMDMs) transfected with shRNA targeting scrambled (Scr) or *SLC31A2* (sh.*SLC31A2*) ($n = 3$). (C and D) Histogram plots and quantification of flow cytometry with MitoSox Red (C) and TMRM (D) staining for measurement of mitochondrial reactive oxygen species (mtROS) and mitochondrial membrane potential (Δψm) in bone marrow-derived macrophages (BMDMs) with LPS (150 ng/mL) stimuli after transfecting with shRNA targeting scrambled (Scr) or *SLC22A5* (sh.*SLC22A5*) ($n = 3$). (E and F) Histogram plots and quantification of flow cytometry with MitoSox Red (E) and TMRM (F) staining for measurement of mitochondrial reactive oxygen species (mtROS) and mitochondrial membrane potential (Δψm) in bone marrow-derived macrophages (BMDMs) with LPS (150 ng/mL) stimuli after transfecting with shRNA targeting scrambled (Scr) or *SLC31A2* (sh.*SLC31A2*) ($n = 3$). Data are expressed as mean ± s.d. (C–F). Unpaired, two-tailed Student's *t*-test (C–F) was used to calculate the *P* value. (For interpretation of the references to colour in this figure legend, the reader is referred to the Web version of this article.)

macrophages via SLC31A2 and SLC22A5.

To address whether SLC31A2 and SLC22A5 downregulation are responsible for mitophagy inhibition of efferocytotic macrophages by CD47-SIRPα blockade, we employed shRNA duplexes that gave robust *SLC31A2* and *SLC22A5* silencing, respectively (Fig. 6A and B). We found that downregulation of SLC22A5, rather than SLC31A2, was crucial for mitophagy inhibition of macrophage, as mtROS production and Δψm cytosolic mtDNA release were elevated in the *SLC22A5*-silenced but not in *SLC31A2*-silenced BMDMs with LPS stimuli (Fig. 6C–F). The elevation of mtROS production and Δψm in the *SLC22A5*-silenced BMDMs could be reversed by concomitant expression of wild-type SLC22A5, ruling out potential off-target effects (Figs. S9C–E).

We then investigated whether SLC22A5 downregulation is a directeffect resulting from efferocytosis mediated by CD47-SIRPα blockadeor secondary to mitophagy inhibition of efferocytotic macrophages. To approach this, the *SIRPA*^{CKO} BMDMs were transfected with *SLC22A5* shRNA first, and then incubated with apoptotic PMNs in the presence of LPS stimuli. Interestingly, silencing of *SLC22A5* made *SIRPA*^{CKO} BMDMs refractory to the efferocytosis-dependent mtROS production and Δψm elevation (Figs. S10A–C). Nevertheless, mitophagy inhibition by the siRNA-mediated deleting of *PINK1* did not affect *SLC22A5* downregulation in the LPS-stimulated *SIRPA*^{CKO} BMDMs with apoptotic PMNs coincubation (Figs. S10D and E). The *PINK1*-deleted BMDMs also had similar *SLC22A5* mRNA levels to the *PINK1*-intact BMDMs regardless of LPS stimuli (Fig. S10F), suggesting that SLC22A5 downregulation serves a downstream event responsible for mitophagy inhibition of efferocytotic macrophages by CD47-SIRPα blockade under inflammatory circumstances.

3.5. *SLC22A5 is a potential immunotherapeutic target for septic AKI*

Emetine, an alkaloid extracted from the root of ipecac that inhibits carnitine transport through deterring SLC22A5, efficiently thwarts cellular autophagy and manifests anti-infectious activity [37,38]. Exposure of the LPS-stimulated BMDMs to emetine increased mtROS production that could be abrogated by silencing SLC22A5 (Fig. 7A and B). The emetine-inducible mtROS production under LPS stimuli was further enhanced in response to different mitophagy inhibitors, including 3-Methyladenine (3-MA), Mdivi-1 and Apigenin

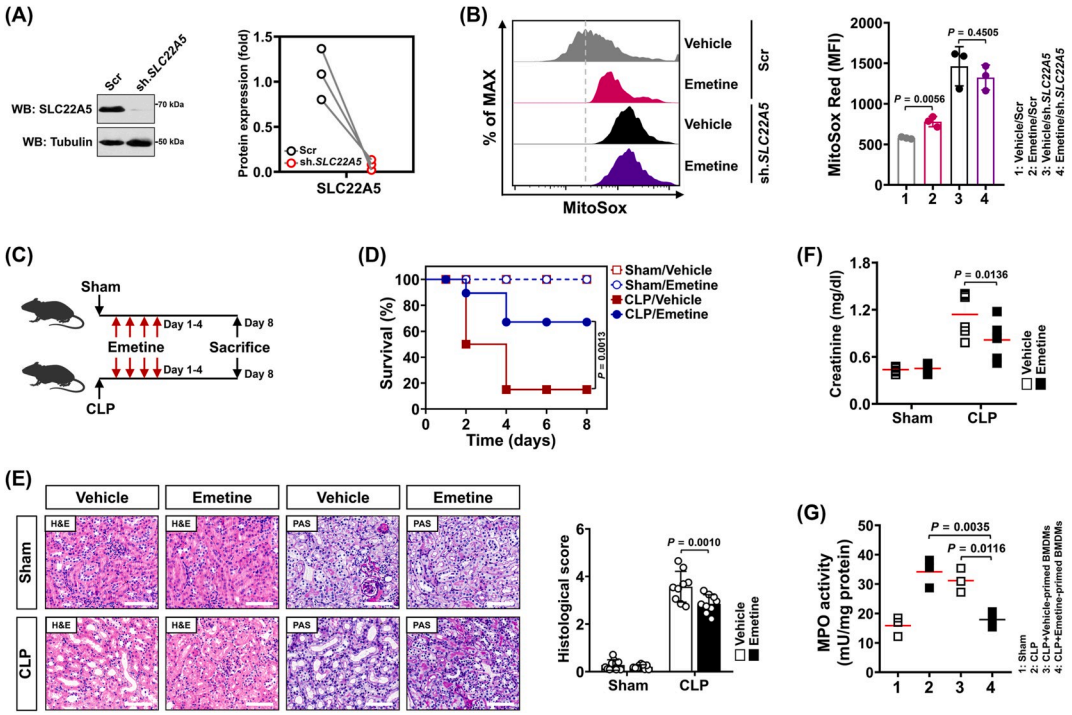

Fig. 7. SLC22A5 is a potential immunotherapeutic target for septic AKI. (A) Western-blotting (WB) analyses determining SLC22A5 abundance in bone marrow-derived macrophages (BMDMs) transfected with shRNA targeting scrambled (Scr) or *SLC22A5* (sh.*SLC22A5*) ($n = 3$). (B) Histogram plots and quantification of flow cytometry with MitoSox Red staining for measurement of mitochondrial reactive oxygen species (mtROS) in the LPS-stimulated bone marrow-derived macrophages (BMDMs) transfected with shRNA targeting scrambled (Scr) or *SLC22A5* (sh.*SLC22A5*) in the presence of emetine (150 nmol/L) treatment ($n = 3$). (C) Schematic showing therapeutic regimen of emetine (0.25 mg/kg) in cecal ligature and puncture (CLP)-challenged mice. (D) Kaplan-Meier curves analyzing survivals of emetine-treated mice with sham and cecal ligature and puncture (CLP) challenge at the indicated times ($n \geq 11$ mice per group). (E) Representative hematoxylin and eosin (H&E) and periodic acid-Schiff (PAS) images and quantification of renal sections from emetine-treated mice with sham and cecal ligature and puncture (CLP) challenge ($n = 9$). Scale bar = 50 μm. (F) Serum creatinine of emetine-treated mice with sham and cecal ligature and puncture (CLP) challenge ($n = 6$). (G) Myeloperoxidase (MPO) activity of kidneys in CLP mice receiving the vehicle- or emetine-primed BMDMs reconstitution after eliminating macrophages ($n = 3$). Data are expressed as mean ± s.d. (B and E-G). Log-rank *t*-test (D) and Two-sided ANOVA with Bonferroni post hoc *t*-test correction (B and E-G) were used to calculate the *P* value. (For interpretation of the references to colour in this figure legend, the reader is referred to the Web version of this article.)

(Fig. S11A). These results suggest that the mitophagy-inhibitory effect of emetine in macrophages under inflammatory stress reply on SLC22A5.

Given that CD47-SIRPα blockade alleviates septic AKI and downregulates SLC22A5 in efferocytotic macrophages, SLC22A5 might be a promising immunotherapeutic target for septic AKI. To address this issue, emetine were administered by oral gavage twice daily for 4 consecutive days into mice with CLP surgery (Fig. 7C). Emetine treatment resulted in reduced mortality as compared with vehicle treatment (Fig. 7D). CLP mice receiving emetine therapy exhibited improved renal morphology with significantly alleviated tubulotoxicity than CLP mice receiving vehicle therapy (Fig. 7E). Biochemical detection revealed that the CLP-challenged mice with emetine treatment had decreased serum creatinine levels compared to the challenged mice with vehicle treatment (Fig. 7F). We then administered emetine to LIE mice and observed that the overwhelming majority of the vehicle-treated mice died within 48 h after LIE challenge, while more than 60% of the emetine-treated mice survived the entire period of endotoxin shock (Figs. S11B and C). LIE mice treated with emetine had markedly ameliorated AKI with respect to sepsis, as indicated by the reduced tubular damage and serum creatinine levels (Figs. S11D and E).

Finally, we asked whether targeting SLC22A5 would affect the anti-septic AKI efficacy of macrophages *in vivo*. To approach this, we eliminated macrophages in mice by clodronate liposome and reconstituted these mice with BMDMs that were primed with emetine, followed by CLP surgery. Renal tissues of the

macrophage-eliminated mice receiving reconstitution of the emetine-primed BMDMs had lower MPO activity than those of the eliminated mice receiving vehicle-primed BMDMs reconstitution (Fig. 7G). These results demonstrate that targeting SLC22A5 potentiates the anti-septic AKI efficacy of macrophages.

4. Discussion

Apoptotic PMNs cause an imbalance in inflammation-immune response, driving unwarranted tissue damage after pathogenic insults. Effective clearance of apoptotic PMNs by innate and adaptive immune systems is a prerequisite for inflammation resolution and injury repair [39]. Although clearance of cell fragments by macrophages is helpful to resolve inflammation, the mechanism underlying efferocytosis towards apoptotic PMNs might be distinct from that underlying phagocytosis towards foreign materials. It is noteworthy that efferocytosis enables metabolic reprogramming and phenotypic conversion in macrophages [40], and recent studies have started to explore the separate roles of efferocytosis and mitophagy in macrophage polarization [41,42]. However, the intrinsic linkage between efferocytosis and mitophagy in pathogenesis of septic AKI remains hitherto undefined. We provide demonstration here that CD47 signalling through SIRPα represents a regulatory loop whereby efferocytosis favors mitophagy inhibition of macrophages through repressing *SLC22A5* transcription, thus reinforcing tubular protection against infectious patterns. More importantly, our study underscores the significance of targeting macrophagic SLC22A5 as a feasible strategy in murine models of septic AKI. Our future work will aim at ascertaining whether other members of carnitine transporter family are responsible for repressing macrophage mitophagy during septic AKI and surmising the precise mechanism of how the CD47-SIRPα blockade-dependent efferocytosis orchestrates *SLC22A5* transcription.

The current paradigm illustrated for mitophagy inhibition of efferocytotic macrohages emphasizes the interaction between CD47 and its receptor SIRPα. Proof-of-concept studies using *SIRPA*-null mice or CD47 and SIRPα blocking mAb have shown beneficial against inflammatory diseases including encephalomyelitis, atherosclerosis, osteoarthritis and autoimmune uveitis (EAU), in all of which efferocytosis plays a fundamental role [43–46]. An effective strategy to restrain excessive inflammation must therefore concern the alterations of macrophagic activity to pathogens. To our knowledge, we believe the present study is the first to demonstrate that CD47-based SIRPα recognition regulates mitophagy of efferocytotic macrophages in response to inflammation. In identifying transcriptional downregulation of *SLC22A5* as a predominant mechanism for mitophagy inhibition of efferocytotic macrophages by CD47-SIRPα blockade, we explore if pharmacological targeting of SLC22A5 could prevent septic AKI. Our experimental results show that emetine could inhibit mitophagy of macrophages and enable the anti-septic AKI phenotypes. This work defines SLC22A5 as an innate immune checkpoint that is essential for the macrophage-mediated immunity against sepsis and provides evidence for the immunotherapeutic potential of targeting SLC22A5 with particular promise in the treatment of septic AKI.

Determining the relationship between efferocytosis and macrophage mitophagy within inflammatory microenvironment allows better prediction of patients who lack efficient therapy against sepsis. Based on our observations that blockade of CD47-SIRPα interaction successfully inhibits macrophage mitophagy in efferocytosis coculture systems *in vitro* and in septic mice, and the evidence that mitophagy inhibition in macrophages confer host defense against sepsis [18], we postulate that CD47-SIRPα signalling may provide valuable prediction of therapeutic effectiveness for septic AKI, for which CD47 impairs response to therapies that rely on efferocytic capacity of macrophages. Our strategy proposes that disruption of CD47-SIRPα interaction may have a prominent advantage over conventional options to cure septic AKI, as the progression of sepsis is an extremely complex pathophysiological process that engages in crosstalk of multiple immune populations, targeting single molecule may have limited efficacy. By providing pre-clinical evidence for the significance of disrupting CD47-SIRPα interaction in protection against septic AKI, our data suggest that additional approach that manipulates this cascade deserves to be further explored in therapeutic regimen of patients with septic AKI.

The contribution of mitophagy to cell fate is controversial ever since it was discovered. Mitophagy is found to be boosted in damaged dopaminergic neurons, lung epithelial cells and tubules [47–49], whereas emerging studies demonstrate that under inflammatory circumstances, mitophagy flux is terminated in various cell types, including adipocytes, T cells and macrophages [50–52]. Mitophagy is associated with glycolytic metabolic shift, $\Delta\psi m$ remodeling, ATP synthesis switch, reduction of mtROS production and cytosolic mtDNA leakage that are required for dealing with the energetic cost of inflammation and ensuring cellular integrity and plasticity. Mitophagy is known to be regulated by the PTEN-induced kinase 1/parkin RBR E3 ubiquitin protein ligase (PINK1/Parkin),

BCL2 and adenovirus E1B 19-kDa-interacting protein 3 (BNIP3), BNIP3-like (BNIP3L/NIX) pathways and dynamin-1-like protein (DRP1) [53–55]. Given the involvement of efferocytosis in inflammation resolution, the pleitropic aspect of macrophages in sepsis and the suspecting reports about the controversial roles of mitophagy, we investigate the correlation of macrophage mitophagy with the anti-septic AKI efficacy of CD47-SIRPα blockade and observe that conditional *SIRPA* knockout renders mitophagy inhibition of efferocytic macrophages and potentiates their abilities to alleviate septic AKI. Our findings highlight the notion that compartmentalized witness of mitophagy might govern distinct homeostatic functions that can be harnessed by the anti-sepsis immunotherapy.

One limitation of the current study is that albeit our study clearly demonstrates that CD47-SIRPα blockade prevents septic AKI via inhibiting mitophagy of efferocytic macrophages through transcriptional downregulation of SLC22A5, the precise relevance of our findings to clinical patients is still yet unclear. Since L-carnitine transporter expression is believed to be downregulated late in the LPS-elicited inflammation [56], targeting of carnitine transporters might be ineffective in patients at late stages of sepsis. So it would be of interest to prioritise therapies based on empirical data before blindly moving forward clinical trials. Another limitation is that our study did not investigate the impact of efferocytosis towards other pathogenic patterns on mitophagy inhibition of macrophages. In previous studies reported by us and other scholars [25,57], tubular mitophagy are protective against septic AKI, so it is possible that low amounts of ROS are essential for cell survival in that setting. Meanwhile, experimental studies and large clinical trials quite convincingly suggest that antioxidants, including ascorbate, MitoTEMPOL and thymoquinone [58–60], should be recommended for sepsis treatment due to the fact that their use may achieve the anti-apoptotic benefits.

5. Conclusions

In summary, we have shown that efferocytosis towards apoptotic PMNs by CD47-SIRPα blockade fosters mitophagy inhibition of macrophages to maintain the anti-septic AKI immunity via downregulating SLC22A5. Our work unearths an intrinsic interplay between immune checkpoint, metabolism profile and mitophagy program in efferocytic macrophages. On this basis, selectively targeting macrophage SLC22A5 may be a promising approach for septic AKI management. Future studies are needed to investigate the immunological features of septic AKI that may benefit from the emetine-based strategy in combination with conventional therapy. It also warrants to elucidate whether immunotargeting of other carnitine transporters is efficient in improving prognosis.

Data availability

All data associated with our study was not deposited into a publicly available repository. And all data will be made available on request.

Funding

The study was funded by by grants from the Natural Science Foundation of Zhejiang Province (No. LHDMY24H190003 and LQ20H150009 to S.-J.M. and LQ20H150010 to J.-Q.L.); National Natural Scientific Foundation of China (No. 82102242 to S.-J.M. and 82272188 to B.-C.H.).

Ethics statement

Study protocol concerning human subjects was approved by the Clinical Research Ethics Committee of Zhejiang Provincial People's Hospital, Hangzhou Medical College, study number QT2022076. All mice were housed in a standard specific-pathogen-free environment in accordance with institutional and NIH guidelines. Veterinary care and animal protocols were approved by the Animal Care & Use Committee of Hangzhou Medical College, study number 20200179.

CRediT authorship contribution statement

Yu Jia: Writing – review & editing, Writing – original draft, Methodology, Investigation, Conceptualization. **Jun-Hua Li:** Methodology, Formal analysis. **Bang-Chuan Hu:** Resources, Funding acquisition. **Xia Huang:** Methodology, Investigation, Formal analysis. **Xi Yang:** Methodology, Investigation, Formal analysis. **Yan-Yan Liu:** Methodology, Formal analysis. **Juan-Juan Cai:** Resources. **Xue Yang:** Resources. **Jun-Mei Lai:** Resources. **Ye Shen:** Resources. **Jing-Quan Liu:** Funding acquisition. **Hai-Ping Zhu:** Resources. **Xiang-Ming Ye:** Writing – review & editing. **Shi-Jing Mo:** Writing – review & editing, Writing – original draft, Supervision, Resources, Methodology, Funding acquisition, Conceptualization.

Declaration of competing interest

The authors declare that they have no known competing financial interests or personal relationships that could have appeared to influence the work reported in this paper.

Acknowledgments

We thank all investigators and participants of this study for their valuable contributions. We thank Dr. X.-L.D. at Westlake

University for technical support.

Appendix A. Supplementary data

Supplementary data to this article can be found online at https://doi.org/10.1016/j.heliyon.2024.e26791.

References

[1] C. Ronco, R. Bellomo, J.A. Kellum, Acute kidney injury, Lancet 394 (2019) 1949–1964.
[2] R. Bellomo, J.A. Kellum, C. Ronco, R. Wald, J. Martensson, M. Maiden, S.M. Bagshaw, N.J. Glassford, Y. Lankadeva, S.T. Vaara, A. Schneider, Acute kidney injury in sepsis, Intensive Care Med. 43 (2017) 816–828.
[3] Y. Jiao, T. Zhang, C. Zhang, H. Ji, X. Tong, R. Xia, W. Wang, Z. Ma, X. Shi, Exosomal miR-30d-5p of neutrophils induces M1 macrophage polarization and primes macrophage pyroptosis in sepsis-related acute lung injury, Crit. Care 25 (2021) 356.
[4] D.C. Nascimento, P.R. Viacava, R.G. Ferreira, M.A. Damaceno, A.R. Pineros, P.H. Melo, P.B. Donate, J.E. Toller-Kawahisa, D. Zoppi, F.P. Veras, R.S. Peres, L. Menezes-Silva, D. Caetite, A.E.R. Oliveira, I.M.S. Castro, G. Kauffenstein, H.I. Nakaya, M.C. Borges, D.S. Zamboni, D.M. Fonseca, J.A.R. Paschoal, T.M. Cunha, V. Quesniaux, J. Linden, F.Q. Cunha, B. Ryffel, J.C. Alves-Filho, Sepsis expands a CD39(+) plasmablast population that promotes immunosuppression via adenosine-mediated inhibition of macrophage antimicrobial activity, Immunity 54 (2021) 2024–2041 e2028.
[5] A. Singhal, S. Kumar, Neutrophil and remnant clearance in immunity and inflammation, Immunology 165 (2022) 22–43.
[6] I. Kourtzelis, X. Li, I. Mitroulis, D. Grosser, T. Kajikawa, B. Wang, M. Grzybek, J. von Renesse, A. Czogalla, M. Troullinaki, A. Ferreira, C. Doreth, K. Ruppova, L. S. Chen, K. Hosur, J.H. Lim, K.J. Chung, S. Grossklaus, A.K. Tausche, L.A.B. Joosten, N.M. Moutsopoulos, B. Wielockx, A. Castrillo, J.M. Korostoff, U. Coskun, G. Hajishengallis, T. Chavakis, DEL-1 promotes macrophage efferocytosis and clearance of inflammation, Nat. Immunol. 20 (2019) 40–49.
[7] T.N. Bukong, Y. Cho, A. Iracheta-Vellve, B. Saha, P. Lowe, A. Adejumo, I. Furi, A. Ambade, B. Gyongyosi, D. Catalano, K. Kodys, G. Szabo, Abnormal neutrophil traps and impaired efferocytosis contribute to liver injury and sepsis severity after binge alcohol use, J. Hepatol. 69 (2018) 1145–1154.
[8] A.N. Barclay, T.K. Van den Berg, The interaction between signal regulatory protein alpha (SIRPalpha) and CD47: structure, function, and therapeutic target, Annu. Rev. Immunol. 32 (2014) 25–50.
[9] R. Majeti, M.P. Chao, A.A. Alizadeh, W.W. Pang, S. Jaiswal, K.D. Gibbs Jr., N. van Rooijen, I.L. Weissman, CD47 is an adverse prognostic factor and therapeutic antibody target on human acute myeloid leukemia stem cells, Cell 138 (2009) 286–299.
[10] M. Sheng, Y. Lin, D. Xu, Y. Tian, Y. Zhan, C. Li, D.G. Farmer, J.W. Kupiec-Weglinski, B. Ke, CD47-Mediated hedgehog/SMO/GLI1 signaling promotes mesenchymal stem cell immunomodulation in mouse liver inflammation, Hepatology 74 (2021) 1560–1577.
[11] G. Wernig, S.Y. Chen, L. Cui, C. Van Neste, J.M. Tsai, N. Kambham, H. Vogel, Y. Natkunam, D.G. Gilliland, G. Nolan, I.L. Weissman, Unifying mechanism for different fibrotic diseases, Proc. Natl. Acad. Sci. U. S. A. 114 (2017) 4757–4762.
[12] R.M. Saliba, U. Greenbaum, Q. Ma, S.A. Srour, Y. Carmazzi, L. Li, B. Oran, M. Moller, J. Wood, S.O. Ciurea, P. Kongtim, G. Rondon, D. Partlow, D. Li, K. Rezvani, E.J. Shpall, K. Cao, R.E. Champlin, J. Zou, Mismatch in SIRPalpha, a regulatory protein in innate immunity, is associated with chronic GVHD in hematopoietic stem cell transplantation, Blood Adv 5 (2021) 3407–3417.
[13] H.C. Tao, K.X. Chen, X. Wang, B. Chen, W.O. Zhao, Y. Zheng, Y.G. Yang, CD47 deficiency in mice exacerbates chronic fatty diet-induced steatohepatitis through its role in regulating hepatic inflammation and lipid metabolism, Front. Immunol. 11 (2020) 148.
[14] D. Rao, K.L. O'Donnell, A. Carmody, I.L. Weissman, K.J. Hasenkrug, A. Marzi, CD47 expression attenuates Ebola virus-induced immunopathology in mice, Antivir. Res. 197 (2022) 105226.
[15] C. Lelubre, J.L. Vincent, Mechanisms and treatment of organ failure in sepsis, Nat. Rev. Nephrol. 14 (2018) 417–427.
[16] J. Sun, J. Zhang, J. Tian, G.M. Virzi, K. Digvijay, L. Cueto, Y. Yin, M.H. Rosner, C. Ronco, Mitochondria in sepsis-induced AKI, J. Am. Soc. Nephrol. 30 (2019) 1151–1161.
[17] H. Amatullah, Y. Shan, B.L. Beauchamp, P.L. Gali, S. Gupta, T. Maron-Gutierrez, E.R. Speck, A.E. Fox-Robichaud, J.L. Tsang, S.H. Mei, T.W. Mak, P.R. Rocco, J. W. Semple, H. Zhang, P. Hu, J.C. Marshall, D.J. Stewart, M.E. Harper, P.C. Liaw, W.C. Liles, C.C. Dos Santos, G. Canadian critical care translational biology, DJ-1/PARK7 impairs bacterial clearance in sepsis, Am. J. Respir. Crit. Care Med. 195 (2017) 889–905.
[18] D. Patoli, F. Mignotte, V. Deckert, A. Dusuel, A. Dumont, A. Rieu, A. Jalil, K. Van Dongen, T. Bourgeois, T. Gautier, C. Magnani, N. Le Guern, S. Mandard, J. Bastin, F. Djouadi, C. Schaeffer, N. Guillaumot, M. Narce, M. Nguyen, J. Guy, A. Dargent, J.P. Quenot, M. Rialland, D. Masson, J. Auwerx, L. Lagrost, C. Thomas, Inhibition of mitophagy drives macrophage activation and antibacterial defense during sepsis, J. Clin. Invest. 130 (2020) 5858–5874.
[19] M. Singer, C.S. Deutschman, C.W. Seymour, M. Shankar-Hari, D. Annane, M. Bauer, R. Bellomo, G.R. Bernard, J.D. Chiche, C.M. Coopersmith, R.S. Hotchkiss, M. M. Levy, J.C. Marshall, G.S. Martin, S.M. Opal, G.D. Rubenfeld, T. van der Poll, J.L. Vincent, D.C. Angus, The third international consensus definitions for sepsis and septic shock (Sepsis-3), JAMA 315 (2016) 801–810.
[20] K.C. Participants, Genetics in chronic kidney disease: conclusions from a kidney disease: improving global outcomes (KDIGO) controversies conference, Kidney Int. 101 (2022) 1126–1141.
[21] Y. Ni, G.H. Wu, J.J. Cai, R. Zhang, Y. Zheng, J.Q. Liu, X.H. Yang, X. Yang, Y. Shen, J.M. Lai, X.M. Ye, S.J. Mo, Tubule-mitophagic secretion of SerpinG1 reprograms macrophages to instruct anti-septic acute kidney injury efficacy of high-dose ascorbate mediated by NRF2 transactivation, Int. J. Biol. Sci. 18 (2022) 5168–5184.
[22] B.C. Hu, J.W. Zhu, G.H. Wu, J.J. Cai, X. Yang, Z.Q. Shao, Y. Zheng, J.M. Lai, Y. Shen, X.H. Yang, J.Q. Liu, R.H. Sun, H.P. Zhu, X.M. Ye, S.J. Mo, Auto- and paracrine rewiring of NIX-mediated mitophagy by insulin-like growth factor-binding protein 7 in septic AKI escalates inflammation-coupling tubular damage, Life Sci. 322 (2023) 121653.
[23] B.C. Hu, G.H. Wu, Z.Q. Shao, Y. Zheng, J.Q. Liu, R. Zhang, J. Hong, X.H. Yang, R.H. Sun, S.J. Mo, Redox DAPK1 destabilizes Pellino1 to govern inflammation-coupling tubular damage during septic AKI, Theranostics 10 (2020) 11479–11496.
[24] Y. Ni, B.C. Hu, G.H. Wu, Z.Q. Shao, Y. Zheng, R. Zhang, J. Jin, J. Hong, X.H. Yang, R.H. Sun, J.Q. Liu, S.J. Mo, Interruption of neutrophil extracellular traps formation dictates host defense and tubular HOXA5 stability to augment efficacy of anti-Fn14 therapy against septic AKI, Theranostics 11 (2021) 9431–9451.
[25] Z.D. Chen, B.C. Hu, X.P. Shao, J. Hong, Y. Zheng, R. Zhang, Z.Q. Shao, J.Q. Liu, X.H. Yang, R.H. Sun, S.J. Mo, Ascorbate uptake enables tubular mitophagy to prevent septic AKI by PINK1-PARK2 axis, Biochem. Biophys. Res. Commun. 554 (2021) 158–165.
[26] S.J. Mo, W. Zhang, J.Q. Liu, M.H. Chen, L. Xu, J. Hong, Q. Li, X.H. Yang, R.H. Sun, B.C. Hu, Regulation of Fn14 stability by SCF(Fbxw7alpha) during septic acute kidney injury, Am. J. Physiol. Ren. Physiol. 316 (2019) F1273–F1281.
[27] J. Hong, B.C. Hu, L. Xu, Y. Zheng, Z.Q. Shao, R. Zhang, X.H. Yang, R.H. Sun, S.J. Mo, MicroRNA-19a targets fibroblast growth factor-inducible molecule 14 and prevents tubular damage in septic AKI, Anal. Cell Pathol. 2020 (2020) 2894650.
[28] O. Tabone, M. Mommert, C. Jourdan, E. Cerrato, M. Legrand, A. Lepape, B. Allaouchiche, T. Rimmele, A. Pachot, G. Monneret, F. Venet, F. Mallet, J. Textoris, Endogenous retroviruses transcriptional modulation after severe infection, trauma and burn, Front. Immunol. 9 (2018) 3091.
[29] X. Qiu, J. Li, J. Bonenfant, L. Jaroszewski, A. Mittal, W. Klein, A. Godzik, M.G. Nair, Dynamic changes in human single-cell transcriptional signatures during fatal sepsis, J. Leukoc. Biol. 110 (2021) 1253–1268.

[30] V.D. Cuevas, M. Simon-Fuentes, E. Orta-Zavalza, R. Samaniego, P. Sanchez-Mateos, M. Escribese, F.J. Cimas, M. Bustos, M. Perez-Diego, A. Ocana, A. Dominguez-Soto, M.A. Vega, A.L. Corbi, The gene signature of activated M-CSF-primed human monocyte-derived macrophages is IL-10-dependent, J. Innate Immun. 14 (2022) 243–256.
[31] M. Antonelou, E. Michaelsson, R.D.R. Evans, C.J. Wang, S.R. Henderson, L.S.K. Walker, R.J. Unwin, A.D. Salama, R.-I. Investigators, Therapeutic myeloperoxidase inhibition attenuates neutrophil activation, ANCA-mediated endothelial damage, and crescentic GN, J. Am. Soc. Nephrol. 31 (2020) 350–364.
[32] A.C. Doran, A. Yurdagul Jr., I. Tabas, Efferocytosis in health and disease, Nat. Rev. Immunol. 20 (2020) 254–267.
[33] C. Nathan, A. Cunningham-Bussel, Beyond oxidative stress: an immunologist's guide to reactive oxygen species, Nat. Rev. Immunol. 13 (2013) 349–361.
[34] D. Engelbertsen, A. Autio, R.A.F. Verwilligen, M.A.C. Depuydt, G. Newton, S. Rattik, E. Levinsohn, G. Saggu, P. Jarolim, H. Wang, F. Velazquez, A.H. Lichtman, F.W. Luscinskas, Increased lymphocyte activation and atherosclerosis in CD47-deficient mice, Sci. Rep. 9 (2019) 10608.
[35] M. Lazarou, D.A. Sliter, L.A. Kane, S.A. Sarraf, C. Wang, J.L. Burman, D.P. Sideris, A.I. Fogel, R.J. Youle, The ubiquitin kinase PINK1 recruits autophagy receptors to induce mitophagy, Nature 524 (2015) 309–314.
[36] S. Morioka, J.S.A. Perry, M.H. Raymond, C.B. Medina, Y. Zhu, L. Zhao, V. Serbulea, S. Onengut-Gumuscu, N. Leitinger, S. Kucenas, J.C. Rathmell, L. Makowski, K.S. Ravichandran, Efferocytosis induces a novel SLC program to promote glucose uptake and lactate release, Nature 563 (2018) 714–718.
[37] C.A. Wagner, U. Lukewille, S. Kaltenbach, I. Moschen, A. Broer, T. Risler, S. Broer, F. Lang, Functional and pharmacological characterization of human Na(+)-carnitine cotransporter hOCTN2, Am. J. Physiol. Ren. Physiol. 279 (2000) F584–F591.
[38] Q. Tang, S. Li, L. Du, S. Chen, J. Gao, Y. Cai, Z. Xu, Z. Zhao, K. Lan, S. Wu, Emetine protects mice from enterovirus infection by inhibiting viral translation, Antivir. Res. 173 (2020) 104650.
[39] C.J. Martin, M.G. Booty, T.R. Rosebrock, C. Nunes-Alves, D.M. Desjardins, I. Keren, S.M. Fortune, H.G. Remold, S.M. Behar, Efferocytosis is an innate antibacterial mechanism, Cell Host Microbe 12 (2012) 289–300.
[40] S. Zhang, S. Weinberg, M. DeBerge, A. Gainullina, M. Schipma, J.M. Kinchen, I. Ben-Sahra, D.R. Gius, L. Yvan-Charvet, N.S. Chandel, P.T. Schumacker, E. B. Thorp, Efferocytosis fuels requirements of fatty acid oxidation and the electron transport chain to polarize macrophages for tissue repair, Cell Metabol. 29 (2019) 443–456 e445.
[41] J. Angsana, J. Chen, L. Liu, C.A. Haller, E.L. Chaikof, Efferocytosis as a regulator of macrophage chemokine receptor expression and polarization, Eur. J. Immunol. 46 (2016) 1592–1599.
[42] D. Bhatia, K.P. Chung, K. Nakahira, E. Patino, M.C. Rice, L.K. Torres, T. Muthukumar, A.M. Choi, O.M. Akchurin, M.E. Choi, Mitophagy-dependent macrophage reprogramming protects against kidney fibrosis, JCI Insight (2019) 4.
[43] T. Nishimura, Y. Saito, K. Washio, S. Komori, D. Respatika, T. Kotani, Y. Murata, H. Ohnishi, S. Mizobuchi, T. Matozaki, SIRPalpha on CD11c(+) cells induces Th17 cell differentiation and subsequent inflammation in the CNS in experimental autoimmune encephalomyelitis, Eur. J. Immunol. 50 (2020) 1560–1570.
[44] K.U. Jarr, R. Nakamoto, B.H. Doan, Y. Kojima, I.L. Weissman, R.H. Advani, A. Iagaru, N.J. Leeper, Effect of CD47 blockade on vascular inflammation, N. Engl. J. Med. 384 (2021) 382–383.
[45] Q. Wang, K. Onuma, C. Liu, H. Wong, M.S. Bloom, E.E. Elliott, R.R. Cao, N. Hu, N. Lingampalli, O. Sharpe, X. Zhao, D.H. Sohn, C.M. Lepus, J. Sokolove, R. Mao, C.T. Cisar, H. Raghu, C.R. Chu, N.J. Giori, S.B. Willingham, S.S. Prohaska, Z. Cheng, I.L. Weissman, W.H. Robinson, Dysregulated integrin alphaVbeta3 and CD47 signaling promotes joint inflammation, cartilage breakdown, and progression of osteoarthritis, JCI Insight (2019) 4.
[46] Y. Okunuki, S.J. Tabor, M.Y. Lee, K.M. Connor, CD47 deficiency ameliorates ocular autoimmune inflammation, Front. Immunol. 12 (2021) 680568.
[47] D.A. Sliter, J. Martinez, L. Hao, X. Chen, N. Sun, T.D. Fischer, J.L. Burman, Y. Li, Z. Zhang, D.P. Narendra, H. Cai, M. Borsche, C. Klein, R.J. Youle, Parkin and PINK1 mitigate STING-induced inflammation, Nature 561 (2018) 258–262.
[48] K. Mizumura, S.M. Cloonan, K. Nakahira, A.R. Bhashyam, M. Cervo, T. Kitada, K. Glass, C.A. Owen, A. Mahmood, G.R. Washko, S. Hashimoto, S.W. Ryter, A. M. Choi, Mitophagy-dependent necroptosis contributes to the pathogenesis of COPD, J. Clin. Invest. 124 (2014) 3987–4003.
[49] J. Wang, P. Zhu, R. Li, J. Ren, H. Zhou, Fundc1-dependent mitophagy is obligatory to ischemic preconditioning-conferred renoprotection in ischemic AKI via suppression of Drp1-mediated mitochondrial fission, Redox Biol. 30 (2020) 101415.
[50] F. He, Y. Huang, Z. Song, H.J. Zhou, H. Zhang, R.J. Perry, G.I. Shulman, W. Min, Mitophagy-mediated adipose inflammation contributes to type 2 diabetes with hepatic insulin resistance, J. Exp. Med. 218 (2021).
[51] D.J. Puleston, H. Zhang, T.J. Powell, E. Lipina, S. Sims, I. Panse, A.S. Watson, V. Cerundolo, A.R. Townsend, P. Klenerman, A.K. Simon, Autophagy is a critical regulator of memory CD8(+) T cell formation, Elife 3 (2014).
[52] W.K.E. Ip, N. Hoshi, D.S. Shouval, S. Snapper, R. Medzhitov, Anti-inflammatory effect of IL-10 mediated by metabolic reprogramming of macrophages, Science 356 (2017) 513–519.
[53] T.N. Nguyen, B.S. Padman, M. Lazarou, Deciphering the molecular signals of PINK1/parkin mitophagy, Trends Cell Biol. 26 (2016) 733–744.
[54] J.W. Harper, A. Ordureau, J.M. Heo, Building and decoding ubiquitin chains for mitophagy, Nat. Rev. Mol. Cell Biol. 19 (2018) 93–108.
[55] E.Q. Toyama, S. Herzig, J. Courchet, T.L. Lewis Jr., O.C. Loson, K. Hellberg, N.P. Young, H. Chen, F. Polleux, D.C. Chan, R.J. Shaw, Metabolism. AMP-activated protein kinase mediates mitochondrial fission in response to energy stress, Science 351 (2016) 275–281.
[56] B. Ling, J. Alcorn, LPS-induced inflammation downregulates mammary gland glucose, fatty acid, and L-carnitine transporter expression at different lactation stages, Res. Vet. Sci. 89 (2010) 200–202.
[57] Q. Lin, S. Li, N. Jiang, X. Shao, M. Zhang, H. Jin, Z. Zhang, J. Shen, Y. Zhou, W. Zhou, L. Gu, R. Lu, Z. Ni, PINK1-parkin pathway of mitophagy protects against contrast-induced acute kidney injury via decreasing mitochondrial ROS and NLRP3 inflammasome activation, Redox Biol. 26 (2019) 101254.
[58] Y.R. Lankadeva, R.M. Peiris, N. Okazaki, I.E. Birchall, A. Trask-Marino, A. Dornom, T.A.M. Vale, R.G. Evans, F. Yanase, R. Bellomo, C.N. May, Reversal of the pathophysiological responses to gram-negative sepsis by megadose vitamin C, Crit. Care Med. 49 (2021) e179–e190.
[59] G.S. Supinski, L. Wang, E.A. Schroder, L.A.P. Callahan, MitoTEMPOL, a mitochondrial targeted antioxidant, prevents sepsis-induced diaphragm dysfunction, Am. J. Physiol. Lung Cell Mol. Physiol. 319 (2020) L228–L238.
[60] L.P. Guo, S.X. Liu, Q. Yang, H.Y. Liu, L.L. Xu, Y.H. Hao, X.Q. Zhang, Effect of thymoquinone on acute kidney injury induced by sepsis in BALB/c mice, BioMed Res. Int. 2020 (2020) 1594726.